

Low Reynolds Number

For the low Reynolds number region following the transition to turbulent flow, the proposal of Herring and Mellor (cited in Ref. 8) that the Clauser factor k varies with the displacement-thickness Reynolds number, $U\delta^*/\nu$ may be written as

$$k = k_\infty [1 + (1100\nu/U\delta^*)^2] \quad (25)$$

where ν is the kinematic viscosity of the fluid and k_∞ is the value of k at high Reynolds number. Cebeci and Smith use a value of $k_\infty = 0.0168$. From Eq. (11), where $U\delta^* = C_{cp}F_{wake}$, the Baldwin-Lomax model can be written as

$$k = 0.0168 [1 + (1100\nu/C_{cp}F_{wake})^2] \quad (26)$$

Concluding Remarks

The pertinent formulas are given by Eq. (24) for the variation of C_{kleb} with the modified Clauser pressure-gradient parameter β , by Eq. (14) for the variation of C_{cp} with C_{kleb} , and by Eq. (26) for the variation of the Clauser factor k with low Reynolds number. As presented here, the relations for the Baldwin-Lomax factors have an indirect experimental validity by being derived from the experimentally confirmed velocity similarity laws. Finally, it should be apparent that for boundary layers in pressure gradients, constant values for the Baldwin-Lomax factors are unsatisfactory in satisfying the velocity similarity laws. To approach the same accuracy as the parent Cebeci-Smith method, the Baldwin-Lomax factors should be varied as indicated.

References

- ¹Baldwin, B. S. and Lomax, H., "Thin Layer Approximation and Algebraic Model for Separated Turbulent Flow," AIAA Paper 78-257, 1978.
- ²Visbal, M. and Knight, D., "Evaluation of the Baldwin-Lomax Turbulence Model for Two-Dimensional Shock Wave Boundary Layer Interactions," *AIAA Journal*, Vol. 22, July 1984, pp. 921-928.
- ³Fujiwara, T., Wang, Y.-Y., and Ohmori, Y., "Turbulent Transonic Flow for NACA 0012/RAE 2822 Airfoils under Baldwin-Lomax Model," *Memoirs of the Faculty of Engineering*, Vol. 37, Nagoya Univ., Japan, 1985, pp. 203-218.
- ⁴York, B. and Knight, D., "Calculations of Two-Dimensional Turbulent Boundary Layers Using the Baldwin-Lomax Model," *AIAA Journal*, Vol. 23, Dec. 1985, pp. 1849-1850.
- ⁵Granville, P. S., "A Modified Law of the Wake for Turbulent Shear Flows," *ASME Journal of Fluids Engineering*, Vol. 98, Sept. 1976, pp. 578-580.
- ⁶Moses, H. L., "The Behavior of Turbulent Boundary Layers in Adverse Pressure Gradients," Gas Turbine Laboratory, Massachusetts Institute of Technology, Cambridge, MA, Rept. 73, Jan. 1964.
- ⁷Nash, J. F., "Turbulent-Boundary-Layer Behavior and the Auxiliary Equation," *Recent Developments in Boundary Layer Research*, AGARDograph 97, May 1965, pp. 253-279.
- ⁸Cebeci, T., "Kinematic Eddy Viscosity at Low Reynolds Numbers," *AIAA Journal*, Vol. 11, Jan. 1973, pp. 102-104.

Modification of the Osher Upwind Scheme for Use in Three Dimensions

Kristin A. Hessenius* and Man Mohan Rai†
NASA Ames Research Center
Moffett Field, California

Introduction

THE Osher upwind scheme, developed for the solution of hyperbolic conservation laws, is an upwind, shock-capturing algorithm based on an approximate Riemann solver. Unlike an exact Riemann solver, it uses compression waves to approximate shocks and thereby simplifies the algorithm.^{1,2} In the solution of the Euler equations in one and two dimensions, this scheme is shown to capture strong shocks crisply with transition over two grid points when the grid is aligned with the shock. The scheme was originally introduced as first-order accurate in space and time with explicit time differencing. However, for two-dimensional problems, Chakravarthy and Osher² present a second-order accurate version, while Rai and Chakravarthy³ present an implicit form of the scheme.

Although the scheme has been used extensively in two dimensions, it has been outlined only for three-dimensional use in Ref. 4. As presented in this reference the algorithm is unsuitable for general computations in three dimensions, however, since it requires that the metrics ξ_x , η_x , and ζ_x of the grid transformation are nowhere zero. Two forms of a necessary modification of the scheme for use on a three-dimensional arbitrary grid are described in this Note.

Need for Modification of the Three-Dimensional Osher Scheme

For a complete description of the Osher upwind scheme, the reader is referred to Refs. 1, 2, and 4. The notation in the Note follows that used in these references.

Key to the development of the Osher algorithm is the identification of invariant quantities, generalized Riemann invariants, along each subpath in state space between adjacent grid points (see the schematic in Fig. 1). By definition, Riemann invariants, Ψ , associated with the n th eigenvalue must satisfy

$$\nabla_Q \Psi \cdot r_n(Q) = 0 \quad (1)$$

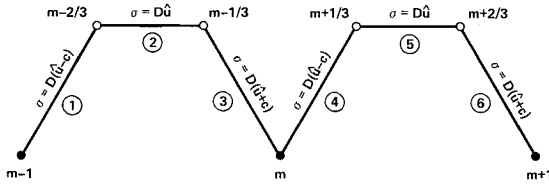
where r_n is the right eigenvector associated with the n th eigenvalue of the flux Jacobian matrices and Q the vector of dependent variables. It may be shown that, given the above definition, the Ψ quantities are invariant along their distinctive subpath.¹ Equation (1) is the only condition necessary to qualify a Riemann invariant.

Figure 1 presents Riemann invariants suggested by Ref. 4 for three-dimensional computations using the Osher scheme. Equating these invariants along their respective subpaths with known values at grid points (for example, $m-1$ and m) produces 10 equations for the 10 unknown quantities at in-

Received Oct. 6, 1986; revision received March 30, 1987. Copyright © 1987 American Institute of Aeronautics and Astronautics, Inc. No copyright is asserted in the United States under Title 17, U.S. Code. The U.S. Government has a royalty-free license to exercise all rights under the copyright claimed herein for Governmental purposes. All other rights are reserved by the copyright owner.

*Assistant Chief, Applied Computational Fluids Branch. Member AIAA.

†Research Scientist, Applied Computational Fluids Branch. Member AIAA.



RIEMANN INVARIANTS ALONG SUBPATHS

① AND ④ : $\hat{u} + \frac{2}{\gamma-1} c, \rho/\rho^\gamma, \hat{v}, \hat{w}$

② AND ⑤ : \hat{u}, ρ

③ AND ⑥ : $\hat{u} - \frac{2}{\gamma-1} c, \rho/\rho^\gamma, \hat{v}, \hat{w}$

WHERE

$$\hat{c} = \left(\frac{\gamma p}{\rho} \right)^{1/2}$$

$$\hat{u} = \frac{k_t + k_x u + k_y v + k_z w}{D}$$

$$\hat{v} = \frac{-k_y u + k_x v}{D}$$

$$\hat{w} = \frac{-k_z u + k_x w}{D}$$

$$D = (k_x^2 + k_y^2 + k_z^2)^{1/2}$$

AND $k = \xi, \eta, \text{ OR } \zeta$ AS APPROPRIATE

Fig. 1 Schematic representation of Osher algorithm with Riemann invariants along subpaths.

intermediate states ($m - 2/3$ and $m - 1/3$). (This discussion assumes an explicit form of the Osher scheme.) Note that should ξ_x, η_x , or ζ_x (the metrics of the grid transformation) be anywhere zero, the Riemann invariants \hat{v} and \hat{w} are no longer linearly independent and the equation set degenerates to 9 linearly independent equations for 10 unknowns. Hence, it is necessary to identify new invariants \hat{v} and \hat{w} that are always independent along subpaths 1, 4, 3, and 6.

Development of New Riemann Invariants

A modified Osher scheme for use in three dimensions on arbitrary grids has been developed and used by the authors to compute the three-dimensional flow over a canard/wing combination using a patched grid system; the results are presented in Ref. 5. Since the completion of this work, however, a simpler approach to the formulation of new Riemann invariants and scheme modification has come to the authors' attention. Because of its elegance this scheme will be presented first.

Assume the following form for \hat{v} and \hat{w} , the new Riemann invariants, where c_i are constants yet to be determined:

$$\hat{v} = c_1 u + c_2 v + c_3 w \quad (2a)$$

$$\hat{w} = c_4 u + c_5 v + c_6 w \quad (2b)$$

Taking the gradient of both \hat{v} and \hat{w} with respect to the dependent variables Q produces the row vectors

$$\nabla_Q \hat{v} = \left[-\left(\frac{c_1}{\rho} u + \frac{c_2}{\rho} v + \frac{c_3}{\rho} w \right), \frac{c_1}{\rho}, \frac{c_2}{\rho}, \frac{c_3}{\rho}, 0 \right] \quad (3a)$$

$$\nabla_Q \hat{w} = \left[-\left(\frac{c_4}{\rho} u + \frac{c_5}{\rho} v + \frac{c_6}{\rho} w \right), \frac{c_4}{\rho}, \frac{c_5}{\rho}, \frac{c_6}{\rho}, 0 \right] \quad (3b)$$

The eigenvector associated with the $\sigma = D(\hat{u} - c)$ subpath (see Fig. 1, σ denotes an eigenvalue) provides the most stringent test for the qualification of a Riemann invariant by Eq. (1)

and may be written as

$$r = \left[-\frac{\rho}{c}, k_x \rho - \frac{\rho}{c} u, k_y \rho - \frac{\rho}{c} v, k_z \rho - \frac{\rho}{c} w, \epsilon \right] \quad (4)$$

where

$$\epsilon = \frac{\rho(u^2 + v^2 + w^2)}{2c} - k_x \rho u - k_y \rho v - k_z \rho w + \frac{\rho c}{(\gamma - 1)}$$

(Note that per Fig. 1, k_x, k_y , and k_z refer to the metrics of the grid transformation with k representing ξ, η , or ζ as appropriate.) From Eq. (1), the following constraints on the constants c_i are derived using Eqs. (3) and (4):

$$c_1 k_x + c_2 k_y + c_3 k_z = 0$$

$$c_4 k_x + c_5 k_y + c_6 k_z = 0 \quad (5)$$

Furthermore, the vectors $[c_1, c_2, c_3]$ and $[c_4, c_5, c_6]$ must be linearly independent to ensure the same for \hat{v} and \hat{w} . In a recent paper by Rogers et al.⁶ on a pseudocompressibility algorithm for the incompressible Navier-Stokes equations, a similar problem in defining linearly independent vectors subject to the constraints of Eq. (5) was encountered. Using their approach to define new Riemann invariants for the three-dimensional Osher scheme, a simple set of c vectors may be derived. For $k = \xi$, we can construct the vectors $[c_1, c_2, c_3]$ and $[c_4, c_5, c_6]$ using reciprocal basis vectors,

$$\begin{pmatrix} c_1 \\ c_2 \\ c_3 \end{pmatrix} = \begin{pmatrix} x_\eta \\ y_\eta \\ z_\eta \end{pmatrix}, \quad \begin{pmatrix} c_4 \\ c_5 \\ c_6 \end{pmatrix} = \begin{pmatrix} x_\zeta \\ y_\zeta \\ z_\zeta \end{pmatrix} \quad (6)$$

The $[c_1, c_2, c_3]$ vector is tangent to the η grid line at a given mesh point, whereas the $[c_4, c_5, c_6]$ vector is tangent to the ζ grid line. Hence the two c vectors are linearly independent. Furthermore, by metric identities, these two vectors are orthogonal to the vector $[\xi_x, \xi_y, \xi_z]$, thereby satisfying Eq. (5). In an analogous way, c vectors may be defined for $k = \eta$ and ζ .

Another way to meet the requirements of Eq. (5) while guaranteeing linear independence of the c vectors is to rotate the $[k_x, k_y, k_z]$ vector to a coordinate axis in xyz space and choose the other two coordinate axes as the transformed c vectors. This is the approach taken by the present authors. For instance, if R is a rotation matrix and

$$R \begin{pmatrix} k_x/D \\ k_y/D \\ k_z/D \end{pmatrix} = \begin{pmatrix} 1 \\ 0 \\ 0 \end{pmatrix}$$

where $D = (k_x^2 + k_y^2 + k_z^2)^{1/2}$, then

$$\begin{pmatrix} c_1 \\ c_2 \\ c_3 \end{pmatrix} = R^{-1} \begin{pmatrix} 0 \\ 1 \\ 0 \end{pmatrix}, \quad \begin{pmatrix} c_4 \\ c_5 \\ c_6 \end{pmatrix} = R^{-1} \begin{pmatrix} 0 \\ 0 \\ 1 \end{pmatrix}$$

Using this approach to derive the constants in the expression for the new Riemann invariants [Eq. (2)], the coefficients c_i are

$$c_1 = \frac{-k_x k_y}{D(k_x^2 + k_z^2)^{1/2}}, \quad c_2 = \frac{(k_x^2 + k_z^2)^{1/2}}{D}, \quad c_3 = \frac{-k_y k_z}{D(k_x^2 + k_z^2)^{1/2}}$$

$$c_4 = \frac{-k_z}{(k_x^2 + k_z^2)^{1/2}}, \quad c_5 = 0, \quad c_6 = \frac{k_x}{(k_x^2 + k_z^2)^{1/2}} \quad (7)$$

The details of the derivation are given in Ref. 5. Note that if both k_x and k_z are zero, certain coefficients are then undefined. This condition is easily remedied by choosing to rotate the given $[k_x/D, k_y/D, k_z/D]$ vector to the "closest" unit axis vector (x, y , or z). This practice will ensure a nonzero denominator in the expressions for the coefficients c_i . (The above expressions are derived by rotating the $[k_x/D, k_y/D, k_z/D]$ vector to a unit vector on the x axis.)

Excluding a redefinition of the invariants \hat{v} and \hat{w} by either of the methods presented in this Note, there are no other required changes to the Osher algorithm for use in general computations. The reader is then referred to Ref. 4 for a more detailed description of the scheme.

References

- ¹Chakravarthy, S. R. and Osher, S., "Numerical Experiments with the Osher Upwind Scheme for the Euler Equations," AIAA Paper 82-0975, June 1982.
- ²Chakravarthy, S. R. and Osher, S., "High Resolution Applications of the Osher Upwind Scheme for the Euler Equations," AIAA Paper 83-1943, June 1983.
- ³Rai, M. M. and Chakravarthy, S. R., "An Implicit Form for the Osher Upwind Scheme," *AIAA Journal*, Vol. 24, May 1986, pp. 735-743.
- ⁴Osher, S. and Chakravarthy, S., "Upwind Schemes and Boundary Conditions with Applications to Euler Equations in General Geometries," *Journal of Computational Physics*, Vol. 50, 1983, pp. 447-481.
- ⁵Hesseniuss, K. and Rai, M. M., "Three-Dimensional, Conservative, Euler Computations using Patched Grid Systems and Explicit Methods," AIAA Paper 86-1081, May 1986.
- ⁶Rogers, S., Chang, J., and Kwak, D., "A Diagonal Algorithm for the Method of Pseudocompressibility," AIAA Paper 86-1060, May 1986.

Entropy Production in Nonsteady General Coordinates

B. M. Argrow,* G. Emanuel,† and M. L. Rasmussen†
University of Oklahoma, Norman, Oklahoma

Introduction

THE second law of thermodynamics is generally not utilized in CFD algorithms, since the law is not essential for obtaining a flowfield solution. However, there are circumstances where the relevance of the second law should not be overlooked. These occur in flows where the entropy production by natural (i.e., irreversible) processes is large, e.g., a chemically reacting boundary layer. For a valid solution, entropy production caused by the algorithm or numerical processes should be small in comparison. There are a variety of sources for numerically produced entropy, including artificial viscosity or damping terms, round-off and truncation errors, and numerical instabilities.

It has become common practice to compute a steady-flow solution by using the nonsteady equations of motion. During the lengthy nonsteady computation, the numerically produced entropy may gradually accumulate. The validity of the computation is then uncertain unless this entropy production, at termination, is still small in comparison to that produced by natural processes.

As an illustration, we have in mind two interesting studies. Both used the nonsteady, conical, Euler equations to asymptotically obtain steady-flow results. (We do not suggest by these remarks that either study is suspect.) One study¹ examined the stability of shock waves attached to wedges or cones. The other² examined the large total pressure loss in a vortical flow on the leeward surface of a swept wing. Entropy production by natural processes is significant in both flows. Nevertheless, it would be useful to know the numerically produced contribution.

As a first step, of course, we need to establish the entropy production of the natural processes. This Note addresses this subject. The determination, however, is not a straightforward task, in part, because the second law is usually formulated as an inequality. This difficulty is avoided by focusing on the rate of entropy production.^{3,4} Because of the complexity of real flows, CFD algorithms often use nonsteady, general, boundary-fitted coordinates. A number of recent publications⁵⁻⁷ have discussed the conservation equations when written in this type of coordinate system. As a supplement to these references, we derive the second law in a corresponding form.

For the purposes of generality, a variety of processes are considered. These include conductive and radiative heat transfer, viscous dissipation, chemical reactions, and molecular diffusion. In the first part of the analysis, the thermodynamic equations are formulated in an invariant form. In the final section, an equation is obtained in the aforementioned coordinate system for the rate of entropy production. This equation is our principle result.

Thermodynamics

A Newtonian fluid in a continuum flow is assumed. The energy equation can be written as³

$$\rho \frac{Dh}{Dt} - \frac{Dp}{Dt} = -\text{div}(q_E + q_R) + \Phi \quad (1)$$

where D/Dt is the substantial derivative, ρ the density, and p the pressure. The specific enthalpy h contains³ the radiative energy density u_R , while the pressure similarly contains a contribution from the radiative stress tensor. Both contributions are almost always negligible⁸ and we neglect these terms in the rest of the discussion. The energy-diffusion flux and radiative heat flux for a mixture of N thermally perfect gases are given by

$$q_E = -k \text{grad } T + \sum_{\alpha=1}^N h_{\alpha} j_{\alpha}$$

$$q_R = \int_0^{\infty} \int_0^{4\pi} I_{\nu} \hat{I} d\Omega d\nu \quad (2)$$

where k is the thermal conductivity, T the temperature, and h_{α} the specific enthalpy of species α . A lengthy constitutive equation for the mass-diffusion flux vector for species α , j_{α} , can be found in Ref. 9. In Eq. (2), I_{ν} is the radiative specific intensity at frequency ν in a differential solid angle $d\Omega$ and the unit vector \hat{I} specifies the direction of propagation of I_{ν} .

The viscous dissipation function Φ in Eq. (1) is the double-dot product of the stress tensor $\vec{\tau}$ with the rate-of-strain tensor $\vec{\epsilon}$,

$$\Phi = \vec{\tau} : \vec{\epsilon} = 2\mu \vec{\epsilon} : \vec{\epsilon} + \lambda (\text{div } V)^2$$

where

$$\vec{\epsilon} = \frac{1}{2} [\text{grad } V + (\text{grad } V)']$$

$$\vec{\tau} = 2\mu \vec{\epsilon} + \lambda (\text{div } V) \vec{I}$$

In these relations, V is the fluid velocity, μ and λ are the first and second coefficients of viscosity, and \vec{I} the unit tensor.

Received April 9, 1987. Copyright © American Institute of Aeronautics and Astronautics, Inc., 1987. All rights reserved.

*Graduate Student. Member AIAA.

†Professor, Aerospace, Mechanical and Nuclear Engineering Department. AIAA Associate Fellow.